PDT Study Using a Model Incorporating Initial Oxygen Concentration and Blood Flow Increase

R. Penjweini[1], and T.C. Zhu[*, 1]
[1] Department of Radiation Oncology, University of Pennsylvania, Philadelphia, Pennsylvania
[*] Corresponding author: tzhu@mail.med.upenn.edu

Abstract: Type II photodynamic therapy (PDT) is an experimental modality for cancer treatment based on the combined action of a photosensitizer, a special wavelength of light and singlet oxygen ($^1O_2$) generation. The cell killing is caused by the reaction of cellular acceptors with $^1O_2$. A mathematical model has been previously developed to incorporate the macroscopic kinetic equations for $^1O_2$ generation, photosensitizers in ground and triplet states, oxygen ($^3O_2$), and tissue acceptors along with the diffusion equation for the light transport in tissue. Accurate estimation of the tissue oxygen changes during PDT is influenced by initial oxygen concentration ($[^3O_2]_0$) and blood flow, so that incorporation of different $[^3O_2]_0$ and blood flow changes in our model allows a better calculation of the $^1O_2$ generation. In this study, the effects of $[^3O_2]_0$, as well as the changes of the blood flow during PDT, on the magnitude of $^1O_2$ generation is studied.

Keywords: Photodynamic therapy, Blood flow, Initial oxygen concentration, Singlet Oxygen, Fluence rate.

1. Introduction

Photodynamic therapy (PDT) is inherently a dynamic process and all key components (photosensitizer, light, and oxygen) interact on time scales relevant to a single treatment [1-5]. The spatial distribution of light in tissue is determined by the light source characteristics and the tissue optical properties (absorption and scattering coefficients) [1, 2, 6, 7]. The tissue optical properties, in turn, are affected by the concentration of photosensitizer, as well as the concentration and oxygenation state of the blood in the tissue [1, 8, 9]. The distribution of oxygen ($^3O_2$) is altered by the photodynamic process, which consumes $^3O_2$, and also by changes of blood content/flow due to vascular damage [1-4, 9]. In type II PDT, the amount of generated singlet oxygen ($^1O_2$) is presumed to be predictive of PDT tissue damage and efficacy. Based on a complete set of kinetic equations, which describe the PDT photochemical processes, a macroscopic model has been developed previously to estimate the concentration of $^1O_2$ generated during PDT and to evaluate the treatment outcome [1, 2, 10, 11]. In this study, several improvements of the model formulations have been made to consider blood flow changes during Photofrin-mediated PDT and to include different initial oxygen concentration ($[^3O_2]_0$) for both tumor and normal tissues.

2. Methods

2.1 Photodynamic equations

By simplifying and combining the energy transfer processes in PDT, a set of equations are produced, which describes the creation of $^1O_2$. These equations are dependent on various parameters such as the light source (*LS*), optical absorption (μ_a) and scattering (μ'_s) coefficients of tissue and photochemical parameters (ξ, σ, g, β) of the photosensitizer [1, 2, 12]. The spatial distribution of light fluence (ϕ) in the tumor is calculated based on the diffusion approximation:

$$\mu_a\phi - \nabla\cdot\left(\frac{1}{3\mu_s'}\nabla\phi\right) = LS \qquad (1)$$

Temporal distribution of photosensitizer (S_0), $^3O_2$ and $^1O_2$ concentrations are obtained by solving a set of coupled time-dependent differential equations [1, 2]:

$$\frac{d[S_0]}{dt} + \left(\xi\sigma\frac{\phi([S_0]+\delta)[^3O_2]}{[^3O_2]+\beta}\right)[S_0] = 0 \qquad (2)$$

$$\frac{d[^3O_2]}{dt} + \left(\xi\frac{\phi[S_0]}{[^3O_2]+\beta}\right)[^3O_2] = g\left(1-\frac{[^3O_2]}{[^3O_2]_0}\right) \qquad (3)$$

$$\frac{d[^1O_2]_{rx}}{dt} - f.\left(\xi\frac{\phi[S_0][^3O_2])}{[^3O_2]+\beta}\right) = 0 \qquad (4)$$

where, $[^1O_2]_{rx}$ is defined as the $^1O_2$ effectively leading cell death. β represents the

ratio of triplet state (T) phosphorescence to reaction between T and $^3O_2$. σ is the ratio of photobleaching to reaction between $^1O_2$ and cellular targets. ξ denotes the initial oxygen consumption rate and δ is the low concentration correction parameter. g is the oxygen perfusion rate to tissue.

For Photofrin-mediated PDT, ξ = 3.7×10^{-3} cm^2 mW^{-1} s^{-1}, β= 11.9 µM, σ = 7.6×10^{-5} μM^{-1}, g = g_0 = 0.7µM/s and δ =33 µM. $[S_0]_0$ = 7 µM and ϕ is considered to be in the range of 25-150 mW/cm^2 [1, 2].

2.2 Simulation of the influence of different $[^3O_2]_0$

Oxygen supply and diffusion into tissues are necessary for survival. The $^3O_2$ partial pressure (pO_2) is a key component of the physiological state of an organ and results from the balance between $^3O_2$ delivery and its consumption [13]. Tissue oxygenation is severely disturbed during pathological conditions such as cancer, which are associated with decrease in pO_2, i.e. 'hypoxia'. pO_2 has been reported to be 30-35 mmHg in solid tumors and 40-50 mmHg in venous blood [13, 14]. Based on these values $^3O_2$ concentration is calculated to be in the range of 40-65 µM.

We have used a broad range of $5<[^3O_2]_0<60$ µM in our simulations to account for the influence of the different $[^3O_2]_0$ as well as hypoxia on our calculations.

2.3 Simulation of blood flow changes during PDT

Oxygen delivery is dependent on the metabolic requirements and functional status of each organ.Due to the PDT oxygen consumption, there is an immediate need for additional $^3O_2$ in tissue. It is reported that the increased $^3O_2$ and nutrient delivery are accomplished by increasing blood flow [15, 16]. The increase of the blood flow has been measured in vivo for MLu-mediated PDT [9]. As shown in Fig. 1-A, in non-sensitized control mice, minor fluctuations in blood flow was detected during illumination. In PDT-treated animals (Fig.1-B), a rapid increase in blood flow occurred during the first 10 minutes of the treatment. It is reported that this increase was consistent among animals, and the peak occurred within the first ~1 to 10 min of treatment. Following the PDT-induced increase, relative blood flow decreased.

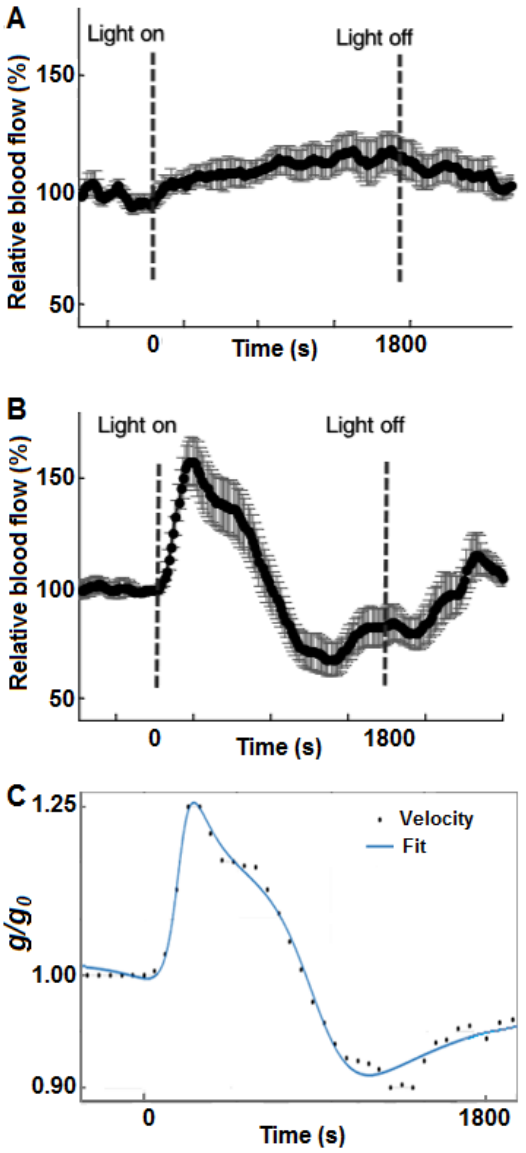

Figure 1. Averaged traces of relative blood flow normalized to pre-illumination values for (A) 10 control mice illuminated without photosensitizer and (B) 15 MLu-PDT treated mice; the illumination performed at 135 J/cm^2 and 75 mW/cm^2. Relative blood flow was calculated as the percentage of the baseline value, measured in the same animal over the 15 min before PDT. The points are the averaged values and the gray bars are standard deviations. (C) Simulated normalized oxygen supply rate; the blue solid line shows the best fit to the data. *Figures A and B are taken from reference [9].*

The published in vivo results have been used in our macroscopic model to simulate the blood flow changes during PDT. For this reason, g was considered to be time dependent. It should also change vs. time similar to blood flow. The g function has been obtained from the best fit to the data in Fig.1-B:

$$g = g_0 \frac{0.99t'^4 + 1.09t'^3 + 0.05t'^2 + 0.18t' + 0.32}{t'^4 + 1.16t'^3 + 0.18t'^2 + 0.24t' + 0.31} \quad (5)$$

where $t' = (t - 750)/632.1$ is normalized by mean 750 and standard deviation 632.1 (with 95% confidence bounds). The temporal changes of normalized g (g/g_0) and the fitting curve to the data have been shown in Fig.1-C.

3. Use of COMSOL Multiphysics

The forward calculation of the macroscopic kinetic equations was done in COMSOL Multiphysics 5.0 for the modeling of $[^3O_2]$ and $[^1O_2]$ generated during PDT. The finite-element-based calculation was implemented within COMSOL by varying the input parameters, such as $[^3O_2]_0$ and ϕ. COMSOL was run on an iMAC OSX version 10.9.5 (Processor 3.1 GHz Intel Core 17 and Memory 16 GB 1600 MHz DDR3). The calculation time was in seconds for coupled differential equations.

4. Results and discussion

A broad range of $5 < [^3O_2]_0 < 60$ µM has been considered in the simulations to investigate the effects of the $[^3O_2]_0$ on the $[^1O_2]$ calculation. Fig. 2 shows the temporal changes of $[^1O_2]$, calculated for three fluence rates of ϕ = 25, 75 and 150 mW/cm^2; PDT treatment time has been considered to be 4000 s. Based on the results, in the well-oxygenated tissue such as 30-60 µM, $[^3O_2]_0$ has low influence on the amounts of calculated $[^1O_2]$. There is maximum 14% difference between $[^1O_2]$ obtained for $[^3O_2]_0$ =30 µM and $[^3O_2]_0$ = 60 µM. When $[^3O_2]_0$ becomes limiting (5-20 µM), small changes in ϕ or $[^3O_2]_0$ have large effects on the generation of $[^1O_2]$.

The effect of the blood flow changes during PDT on the calculation of $[^3O_2]$ and $[^1O_2]$ was investigated. The simulations have been done for ϕ = 75 mW/cm^2 and well-oxygenated conditions, when $30 < [^3O_2]_0 < 60$ µM. The temporal changes of normalized g to g_0 has been shown in Fig. 3.

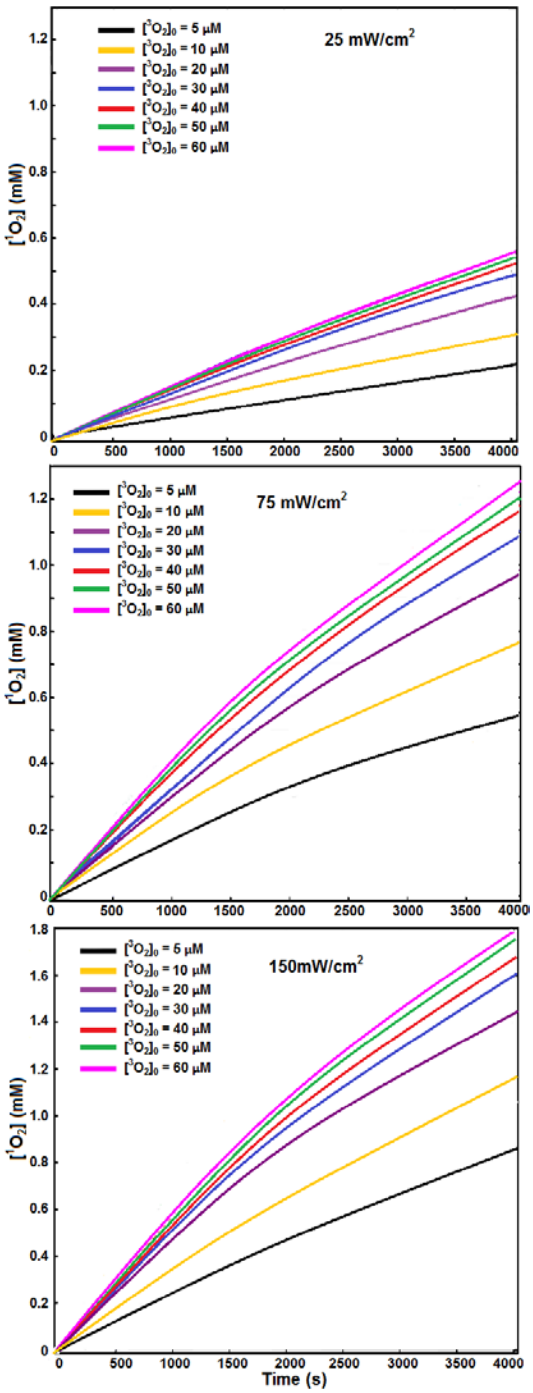

Figure 2. Temporal changes of the singlet oxygen concentration ($[^1O_2]$) calculated for initial oxygen concentration ($[^3O_2]_0$) ranges from 5 to 60 µM and fluence rates of 25, 75 and 150 mW/cm^2.

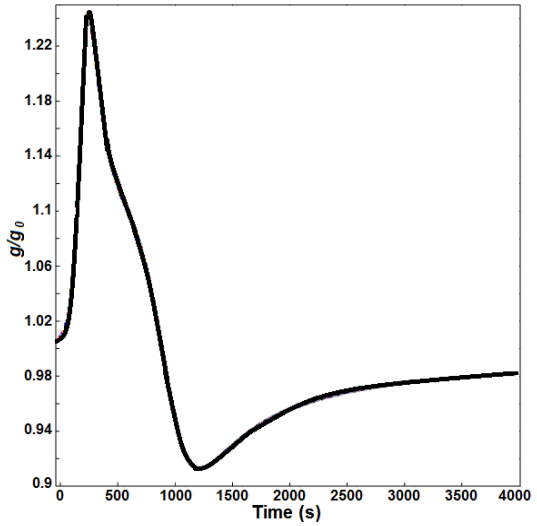

Figure 3. Temporal changes of the normalized g to g_0 during PDT. The simulation has been done for light fluence 75 mW/cm^2.

Fig. 4-A shows the temporal changes of $[^3O_2]$ for different $[^3O_2]_0$. The dashed lines show the results obtained without considering blood flow changes and the solid lines show the amounts of $[^3O_2]$ calculated with the model incorporating the blood flow changes. Based on the calculation results, there is an immediate drop of $[^3O_2]$ at the beginning of the treatment (within 100-150 s). In the model, which includes blood flow changes during PDT (see solid lines), $[^3O_2]$ increases slightly after ~ 100 s and it reaches ~ 77%, 67%, 56% and 0.45% of its initial value for $[^3O_2]_0$ = 60, 50, 40 and 30 µM, respectively. This oxygen recovery might be due to the increased $^3O_2$ delivery accomplished by increasing blood flow. In the model that does not consider the blood flow changes, $[^3O_2]$ (dashed lines) shows a sharper decrease and less recovery at the beginning of PDT. After about 1200 s, $[^3O_2]$ shows the same recovery behavior for the two models.

The singlet oxygen concentration has been calculated by using the model incorporating the blood flow changes. Fig. 4-B presents the results of the calculation for $[^3O_2]_0$ = 30, 40, 50 and 60 µM. The amounts of $[^1O_2]$ has been compared with those calculated without blood flow changes, which shows a close agreement between the two models. This close agreement might be due to the similar average $[^3O_2]$ obtained by the two models.

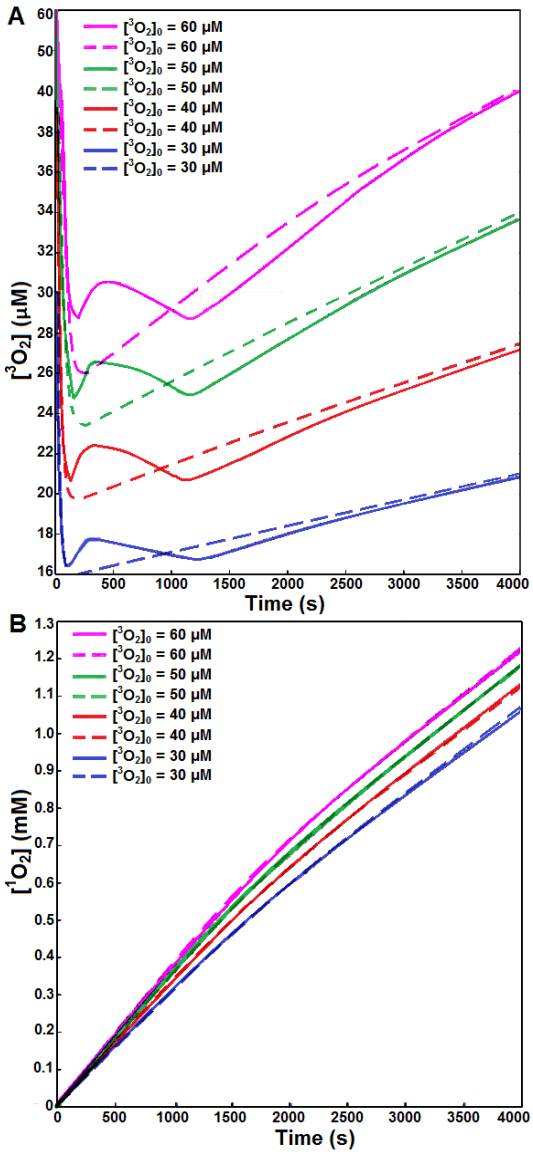

Figure 4. Temporal changes of (A) oxygen concentration ($[^3O_2]$), (B) singlet oxygen concentration ($[^1O_2]$). The solid lines present the data obtained by using the macroscopic model incorporating blood flow changes during PDT. The dashed lines show the amounts of $[^3O_2]$ and $[^1O_2]$ without considering blood flow changes. Initial oxygen concentrations ($[^3O_2]_0$) ranges from 30 to 60 µM. The fluence rate is considered to be 75 mW/cm^2.

6. Conclusions

The model formulations have been improved to consider $[^3O_2]_0$ for both tumor and normal tissues during PDT. The simulation results show

that in the well-oxygenated tissue, the exact estimation of $[^3O_2]_0$ will have little influence on treatment efficacy. When the amounts of $[^3O_2]_0$ becomes limiting, small changes in ϕ or $[^3O_2]_0$ have large effects on the generation of $[^1O_2]$. The same amount of $[^1O_2]$ was calculated by using the model incorporating blood flow changes. However, modeling of the blood flow changes during PDT will be further improved based on our future in vivo mice studies.

7. Acknowledgements

This work is supported by National Institute of Health (NIH) P01 CA87971 and R01 CA 154562 grants. We are grateful for helpful discussions with and insights from Dr. Jarod C. Finlay.

8. References

[1] T.C. Zhu, B. Liu, R. Penjweini, Study of tissue oxygen supply rate in a macroscopic photodynamic therapy singlet oxygen model, Journal of biomedical optics, **20**, 38001 (2015).
[2] K.K. Wang, J.C. Finlay, T.M. Busch, S.M. Hahn, T.C. Zhu, Explicit dosimetry for photodynamic therapy: macroscopic singlet oxygen modeling, Journal of biophotonics, **3**, 304-318 (2010).
[3] T.M. Busch, H.W. Wang, E.P. Wileyto, G. Yu, R.M. Bunte, Increasing damage to tumor blood vessels during motexafin lutetium-PDT through use of low fluence rate, Radiation research, **174**, 331-340 (2010).
[4] Q. Chen, H. Chen, F.W. Hetzel, Tumor oxygenation changes post-photodynamic therapy, Photochemistry and photobiology, **63**, 128-131 (1996).
[5] J.C. Finlay, A. Darafsheh, "Light sources, drugs, and dosimetry," in Biomedical optics in otorhinolaryngology, head and neck surgery: principles and practices, B. Wang and J. Ilgner, Eds., Springer (2015).
[6] J. Li, T.C. Zhu, J.C. Finlay, Study of light fluence rate distribution in photodynamic therapy using finite-element method, Proc. SPIE, **6139**, 61390M (2006).
[7] A. Dimofte, J.C. Finlay, T.C. Zhu, A method for determination of the absorption and scattering properties interstitially in turbid media, Physics in medicine and biology, **50**, 2291-2311 (2005).
[8] T.C. Zhu, J.C. Finlay, The role of photodynamic therapy (PDT) physics, Medical physics, **35**, 3127-3136 (2008).
[9] G. Yu, T. Durduran, C. Zhou, H.W. Wang, M.E. Putt, H.M. Saunders, C.M. Sehgal, E. Glatstein, A.G. Yodh, T.M. Busch, Noninvasive monitoring of murine tumor blood flow during and after photodynamic therapy provides early assessment of therapeutic efficacy, Clinical cancer research: an official journal of the American Association for Cancer Research, **11**, 3543-3552 (2005).
[10] K.K. Wang, T.C. Zhu, Explicit dosimetry for photodynamic therapy; singlet oxygen modeling based on finite-element method, Proceedings of COMSOL (2009).
[11] X. Liang, K.K. Wang, T.C. Zhu, Parameter optimization for FEM based modeling of singlet oxygen during PDT using COMSOL, Proceeding of the COMSOL (2010).
[12] X.H. Hu, Y. Feng, J.Q. Lu, R.R. Allison, R.E. Cuenca, G.H. Downie, C.H. Sibata, Modeling of a type II photofrin-mediated photodynamic therapy process in a heterogeneous tissue phantom, Photochemistry and photobiology, **81**, 1460-1468 (2005).
[13] A. Carreau, B. El Hafny-Rahbi, A. Matejuk, C. Grillon, C. Kieda, Why is the partial oxygen pressure of human tissues a crucial parameter? Small molecules and hypoxia, Journal of cellular and molecular medicine, **15**, 1239-1253 (2011).
[14] M. Hockel, P. Vaupel, Tumor hypoxia: definitions and current clinical, biologic, and molecular aspects, Journal of the National Cancer Institute, **93**, 266-276 (2001).
[15] Korthuis, R.J. Skeletal muscle circulation, Chapter4: Exercise hyperemia and regulation. San Rafael (CA); Morgen & Claypool Life Sciences (2011).
[16] Pittman R.N. Regulation of Tissue Oxygenation. Matching oxygen suppply to oxygen demand. Chapter 8. San Rafael (CA); Morgen & Claypool Life Sciences (2011).